I give permission for public access to my thesis and for copying to be done at the discretion of the archives' librarian and/or the College library.

Signature Date

THE ROLE OF DROSOPHILA INHIBITOR OF APOPTOSIS (*DIAP1*) IN FAT BODY REMODELING

by

Anne Sarie Yva Cossogue

A Paper Presented to the

Faculty of Mount Holyoke College in

Partial Fulfillment of the Requirements for

the Degree of Bachelor of Arts with

Honor

Department of Biological Sciences

South Hadley, MA 01075

May, 2012

This paper was prepared
under the direction of
Professor Craig Woodard
for eight credits.

To my father, my mother, my ants, and friends

who made it possible for me

ACKNOWLEDGMENTS

I would like to thank God for all his blessings throughout my undergraduate studies.

I would also like to thank my mentor Dr. Craig Woodard for giving the opportunity to work in his lab. Dr. Woodard had been very supportive throughout the entire academic year and had been very patient, and understanding. Dr. Woodard was always available for me.

Thanks to my second committee member, Dr. Lilian Hsu who helped me design my primers. Dr. Dr. Hsu was also available and willing to help in any possible way. Thanks also to my third committee member, Dr. Mark Peterson for being available for me.

Instructor Marian Rice has been very helpful at teaching me all the fluorescence microscopy techniques. Thanks my lab team for being supportive during this past academic year.

Last, I would like to thank Mount Holyoke College Department of Biological Sciences and HHMI for funding my independent research.

TABLE OF CONTENTS

LIST OF FIGURES

LIST OF TABLES

ABSTRACT

During metamorphosis in *Drosophila melanogaster* some larval tissues are destroyed through programmed cell death (PCD) (Aguila et al., 2007). The steroid hormone 20-hydroxyecdysone (ecdysone) regulates several genes that induce PCD in *Drosophila* (McBrayer et al 2007). Apoptosis, which is a type of PCD, occurs when the antiapoptotic gene *diap1* is downregulated in larval tissues. DIAP1 regulates apoptosis by deactivating caspases (Orme and Meier, 2009). During metamorphosis, the larval fat body, which is composed of a sheet of connected cells, is not destroyed by PCD. This organ is instead remodeled and is transformed into individual, spherical, and loose cells (Nelliot et al., 2006).

I hypothesize that *diap1* is expressed in the larval fat body throughout metamorphosis and that this helps to inhibit PCD in this organ. To test this hypothesis, I examined *diap1* transcript levels in wild type *Drosophila* using qPCR. In addition, I determined the expression of *diap1* in larval fat body of flies with a *diap1* RNAi construct. My results demonstrate that *diap1* is expressed in the larval fat body during prepupal and early pupal development. Preliminary findings showed that *Drosophila* expressing the *diap1* RNAi construct failed to undergo normal fat body remodeling. This finding suggests that *diap1* is necessary for the normal timing of fat body remodeling and the successful development of *Drosophila*.

INTRODUCTION

Programmed Cell Death (PCD)

Programmed Cell Death (PCD) is a controlled mechanism that occurs at specific times and locations during the development of organisms (Jacobson et al., 1997). Cell death can be physiological and under genetic control (as in the case with PCD). Physiological PCD is observed in normal cell development and is important in nervous tissue remodeling, limb formation, and destruction of unwanted tissues (Lee and Baehrecke, 2001). PCD contributes to tissue homeostasis by balancing the number of replicating and dying cells (Gavrieli et al., 1992). Abnormal PCD activity involves immune cell dysfunction, cancer, and neurodegeneration (Debnath et al., 2005). Three different types of PCD are observed in cells: apoptosis, non-lysosomal vesiculate degradation, and autophagic cell death. The depolarization of mitochondrial membrane, the release of cytochrome c, and the presence of caspases are cellular signals that trigger apoptosis. Cells undergoing apoptosis shrink and aggregate while keeping their organelles and plasma membranes intact. They are quickly engulfed by macrophages before degradation. Non-lysosomal vesiculate degradation, on the other hand, involves swelling of the cell's organelles and their degradation (Carke, 1990). Cells that are destroyed by

autophagy contain autophagic vacuoles. They are engulfed by autophagosomes, and are further degraded in the lysosomes. The biomolecules from cells degradation through autophagy are recycled and used by other tissues as nutrients (Scott et al., 2004).

Steroid Regulation in PCD

Drosophila melanogaster (the fruit fly) is a useful model for the study of PCD because it possesses homologs of several mammalian cell death genes. The fly also undergoes developmental events that are similar to those in vertebrates (Lee et al., 2000). Steroid hormones regulate programmed cell death in mammals and insects. Steroids are small lipophilic molecules that are permeable to cell membranes. Steroids bind directly to ligand-regulated transcription factors and provoke signals for PCD (Yin and Thummel, 2004). In mammals, glucocorticoid triggers the cell death of immature thymocytes and T-cells through apoptosis (Thummel, 2007). In *Drosophila melanogaster,* the steroid hormone 20-hydroxyecdysone (ecdysone) triggers PCD to remove some larval tissues that are no longer needed by the adult fly. For instance, the second pulse of ecdysone activates caspases, which induce PCD in the salivary glands around 12 hours after puparium formation (APF) (Lee and Baehrecke, 2001).

Regulation of Ecdysone

Ecdysone regulates several genes that induce specific events such as PCD, tissue remodeling, and imaginal tissue differentiation during the development of *Drosophila*. In order to enter metamorphosis, it is necessary that the larva reaches an adequate size and stores enough nutrients to survive the long non-feeding period. Prothoracicotropic hormone (PTTH) is a neurosecretory hormone released from the brain that triggers ecdysone production and secretion when the larva reaches its critical weight (McBrayer et al., 2007; Riddiford et al., 2003). Consequently, the ring gland, which is located between the two brain hemispheres of the *Drosophila*, releases ecdysone in pulses (fig. 1). Ecdysone is converted to β 20-hydroxyecdysone (20E) by the enzyme ecdysone 20-mono-oxygenase in the fat body (fig. 2). The ring gland is a compound gland that includes the corpus allatum, the thoracic glands, and the corpora cardiaca. The corpus allatum produces juvenile hormone (JH) and the thoracic glands produce ecdysone (Hartenstein, 1993). The ring gland secretes hormones that regulate molting, metamorphosis, and organ growth in *Drosophila* (Demerec, 1950). The same process occurs in the body wall and gut of the tobacco hornworm. Tissues respond to ecdysone through a heterodimeric receptor composed of Ecdysone receptor (EcR) and Ultraspiracle (Usp).

Usp is a nuclear receptor that controls the expression of target genes by binding to small hydrophobic molecules such as 20E (Brennan et al., 2001; Schubiger et al., 1998; Greenwood and Rees, 1984; Maki et al., 2004). In *Drosophila*, molting and metamorphosis are regulated by the JH and ecdysone. Ecdysone directs molting and metamorphosis while JH regulates growth during the larval stage and facilitates the transition of the larva from the first instar to the second and third one. The level of JH decreases as the larva reaches a specific size and enters metamorphosis (Riddiford, 2008).

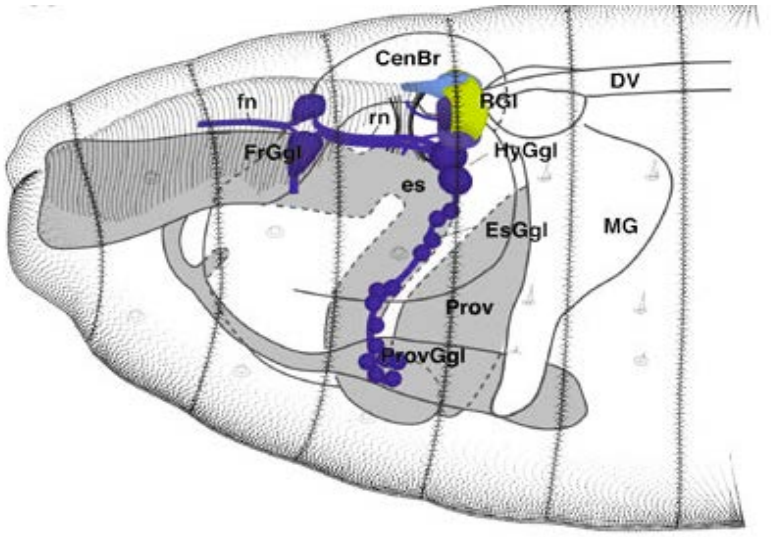

Figure 1. Ring Gland of *Drosophila melanogaster*
The ring gland (RGL), which is shown in green, is located at the end of the dorsal vessel (DV). This ring gland is part of the *Drosophila* embryonic stomatogastric nervous system. The ring gland is composed of three endocrine organs: the corpus allatum, the thoracic glands, and the corpora cardiaca (Hartenstein, 1993).

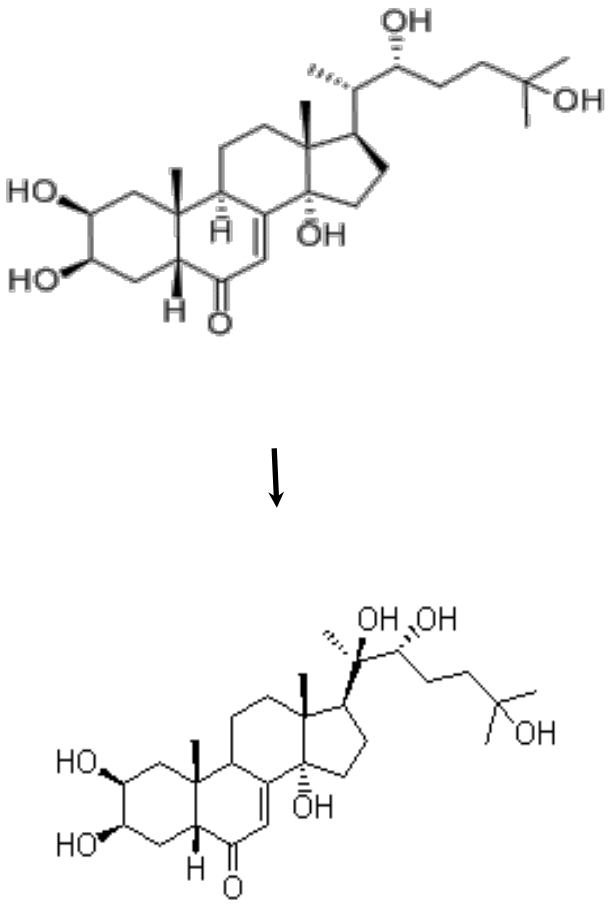

Figure 2. **Conversion of α Ecdysone to β 20-Hydroxyecysone**. α Ecdysone is released from the ring gland and is hydroxylated by the enzyme ecdysone 20-mono-oxygenase in the fat tissue and other target tissues. Ecdysone is derived from cholesterol (Demerec, 1950).

Gene Regulation during Metamorphosis

The life cycle of *Drosophila melanogaster* is divided into four stages: Embryo, larva, pupa, and adult (Aguila et al., 2007) (fig. 3). At the end of the third instar larval stage, the larva stops eating and encases itself into a puparium. The puparium formation is referred to as 0 hour and subsequent developmental stages during metamorphosis are referred to as after puparium formation (APF) (Riddiford, 1993). A fluctuation in the level of the steroid hormone ecdysone directs the beginning of *Drosophila* metamorphosis. Two pulses (peaks in concentration of 20E) occur at different times between 0 and 12 hours after the beginning of metamorphosis. The first pulse of ecdysone induces the transcription of the early genes: *BR-C, E74A,* and *E75A,* which are required for puparium formation. The first pulse occurs at the end of the larval stage and is followed by the expression of *βftz-f1.* ßFTZ-F1 acts as a competence factor that enables certain genes to respond to ecdysone (Woodard et al., 1994). The second pulse of ecdysone, which occurs at around 12 hour (APF), induces the transition between prepupa and pupa. During the prepupal stage, the larva stops moving and encases itself into a puparium. This prepupal to pupal transition is characterized by the eversion of the head, the extension of the wings and legs, and the destruction of the larval salivary glands with the induction of the early genes *BR-C, E74A, E75A* by

the second pulse of ecdysone along with *E93* at 12 hr APF (Bond et al., 2011).

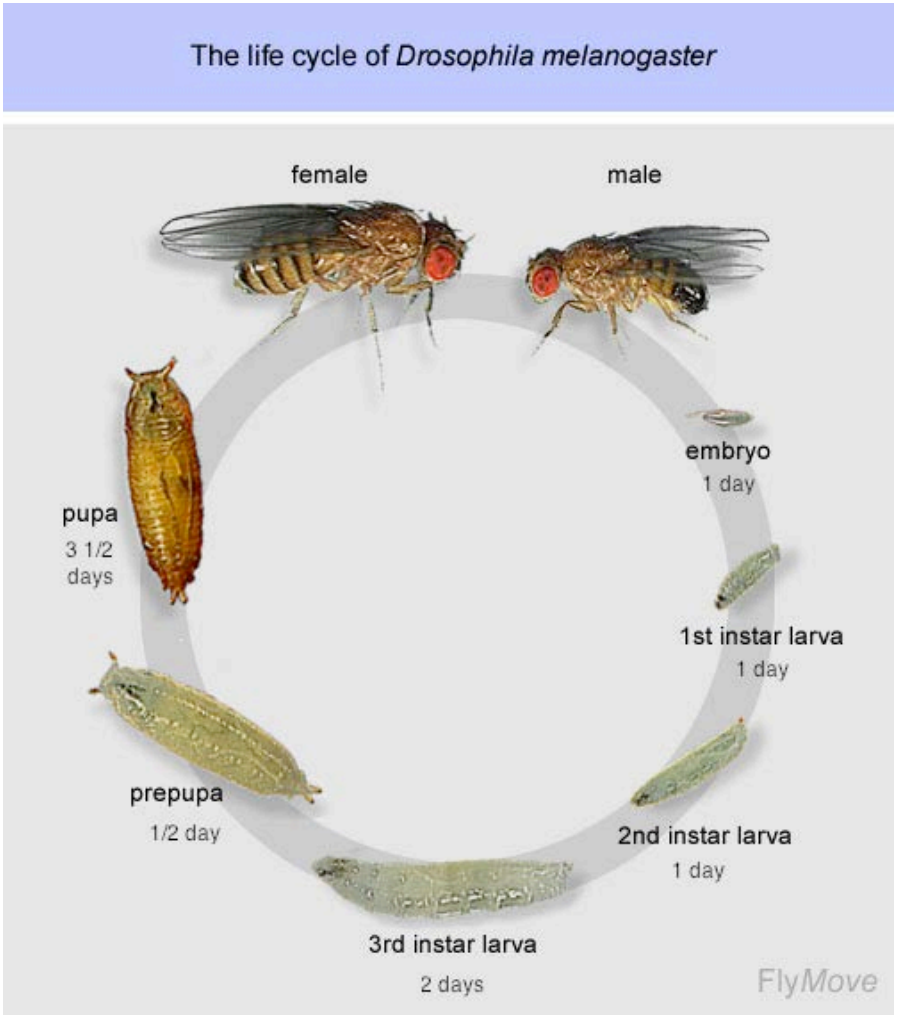

Figure 3. Life cycle of *Drosophila melanogaster*. The life cycle of *Drosophila* includes: embyo, larva, pupa, and adult. After mating with a male, the female fly lays fertilized eggs. The embryo develops into a larva, which crawls and eats constantly for approximately four days. The larval stage is subdivided into first, second, and third instars. *Drosophila* enters metamorphosis at the prepupa stage. At the end of the pupal stage, an adult fly eventually emerges (Flymove; Riddiford, 1993).

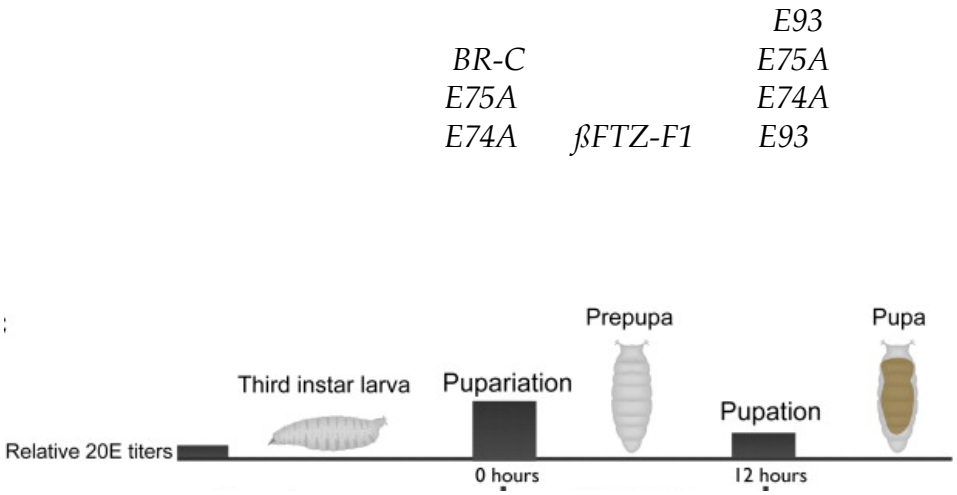

Figure 4. Gene regulation by ecdysone in *Drosophila melanogater* salivary glands. The secretion of the hormone 20 hydroxyecdysone (20E) at around 0 hr APF, marks the beginning of metamorphosis and the induction of the early genes *E74A*, *E75A*, and *BR-C*. As the prepupa progresses through metamorphosis, the level of ecdysone decreases and the competence factor *ßftz-f1* is expressed. At around 12 hr APF, a second pulse of ecdysone occurs and the early genes are re-induced along with *E93* (Bond et al., 2011; Broadus et al., 1999).

Autophagy and Apoptosis Regulation

Autophagy and apoptosis are two common PCD events that occur in organisms during development. Autophagy is triggered in eukaryotic cells during starvation, organelle damage, and cellular remodeling. Autophagy is regulated by the Target of rapamycin (TOR) family of

Serine-Threonine kinases. In yeast, TOR suppresses autophagy during non-starvation periods by regulating the Ser-Thr kinase Atg1 complex and the expression of ATG8. In complex eukaryotes, the insulin/class I phosphoinositide 3-kinase (PI3K), which is located upstream of TOR, suppresses starvation-induced autophagy (Scott et al., 2004; Marino and Lopez-Otin, 2004). PI3K is activated by insulin receptor and insulin receptor substrate proteins when the cells need nutrients (Baerecke, 2005).

Apoptosis on the other hand is controlled by cysteine proteases or caspases. Caspases are activated in three different ways: the oligo-merization of the caspase-8 using a death effector domain, the formation of an intraprocaspase complex by an unknown adaptor protein, and the grouping of caspases into multimers with Apaf-1/CED-4, CARD (caspase recruitment domain) containing nucleotide binding proteins. Mammals and *C. elegans* use Apaf-1 and CED-4 respectively. Both Apaf-1 and CED-4 require ATP-binding site in their NBARC (nucleotide-binding adaptor shared by Apaf-1, certain R gene products, and CED-4) motifs. However, cytochrome c is required for the activation of Apaf-1 (Kanuka et al., 1999).

PCD in *Drosophila* is orchestrated by caspases. The *Drosophila* genome codes for seven capases: DRONC, DREDD, DREAM/STRICA, DCP-1, DRICE, DECAY, and DAYDREAM/DAMM. There are two classes of caspases: class I and class II. Class I caspases contain a long prodomain with protein-protein interaction motifs such as caspase recruitment

domain (CARD) or death effector domain (DEDD) and class II caspases possess a short prodomain. The activation of those caspases triggers apoptosis by cleaving proteins such as dCAD (*Drosophila* caspase-activated DNase). dCAD is a cell death regulatory component and DNase is an enzyme that cleaves DNA (Lee et al., 2002; Kumar and Doumanis, 2000).

However, only DRONC, DCP-1, and DRICE are involved in PCD. Caspases are usually found in the form of zymogens, which are activated in cascades of auto and trans-stimulation. Caspases are activated when the zymogen form is cleaved and assemble into heterotetramers (Kumar, 2007). DARK is an Apaf-1 domain protein that is required for the activation of DRONC. Once activated DRONC cleaves and activates downstream effector caspases to amplify its proteolytic activities (Kumar and Doumanis, 2000).

Apart from the caspases, *Drosophila* also possesses the proteins: DIAP1 (*Drosophila* inhibitor of apoptosis 1), dBRUCE (*Drosophila* BIR repeat containing ubiquitin-conjugating enzyme), and Deterin, which inhibit apoptosis. These inhibitor proteins each possess a Baculovirus IAP repeat (BIR) domain that contains an ubiquitin-conjugating enzyme. DIAP1 contains two BIR repeat domains and a C-terminus Really Interesting New Gene (RING) E3 ligase while dBRUCE and Deterin contain one BIR repeat domain. The BIR1 domain of DIAP1 binds the two

effector caspases DCP-1 and DRICE while the BIR2 domain binds DRONC. Thus, DIAP1 can binds all three caspases at the same time (Orme and Meier, 2009; Kumar and Doumanis, 2000).

In addition to DIAP1, *Drosophila* also possesses four cell death activators: REAPER (rpr), HEAD INVOLUTION DEFECTIVE (hid), GRIM, and SICKLE or IAP antagonists that are involved in PCD. They interact with DIAP1 by controlling its interaction with caspases (Lee et al., 2002).

In order to inhibit apoptosis, DIAP1 requires the proteolytic cleavage of its first 20 amino acid residues, which provides a binding region for UBR-containing E3 ligases. DRONC binds to DIAP1 in its zymogen form while DCP-1 and DRICE require proteolytic cleavage. Upon binding, the caspases are subject to ubiquitylation and are deactivated. However, the IAP-binding motif (IBM) of DCP-1 and DRICE resemble the IBM of the IAP antagonists: RPR, HID, GRIM, and SICKLE. The IBM contains the amino acid residue alanine (ALA) at the first position, which is necessary for the binding of DCP-1 and DRICE to DIAP 1. DRONC also possesses a short internal sequence that is similar to an IBM. To perform its IAP antagonist activity and interact with the BIR domain of DIAP 1, the initiating methionine (MET) of RPR, HID, GRIM, or SICKLE is cleaved to expose the free N-terminus of ALA. When IAP antagonists bind to DIAP1, they trigger DIAP1 auto-ubiquitylation

followed by degradation (Kumar and Doumanis, 2000). Nevertheless, the IAP antagonists bind selectively to the BIR domains of DIAP 1. RPR and GRIM bind to BIR1 and BIR2 domains of DIAP1 with the same affinity while HID and SICKLE bind to BIR2 domains. Thus, IAP antagonists promote PCD by binding to DIAP 1 active site to liberate the caspases and to inhibit their anti-apoptotic activities (Orme and Meier, 2009; Yin et al., 2007).

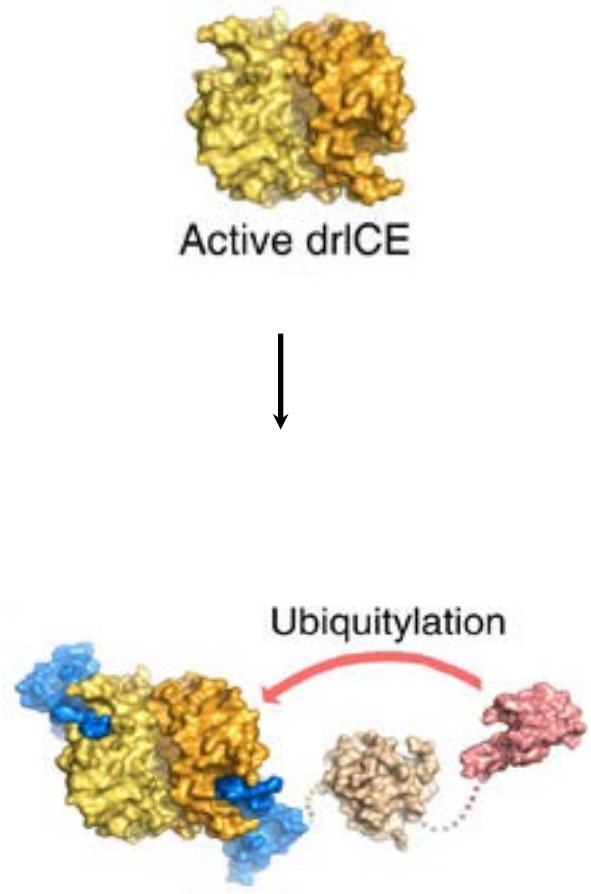

Figure 5. DIAP1-DRICE inhibitory complex. Active DRICE binds to the DIAP1 BIR 1 domain shown in blue. Upon binding, the C-terminus Really Interesting New Gene (RING) tags the caspase for degradation through ubiquitylation (Li et al., 2011; Orme and Meier, 2009).

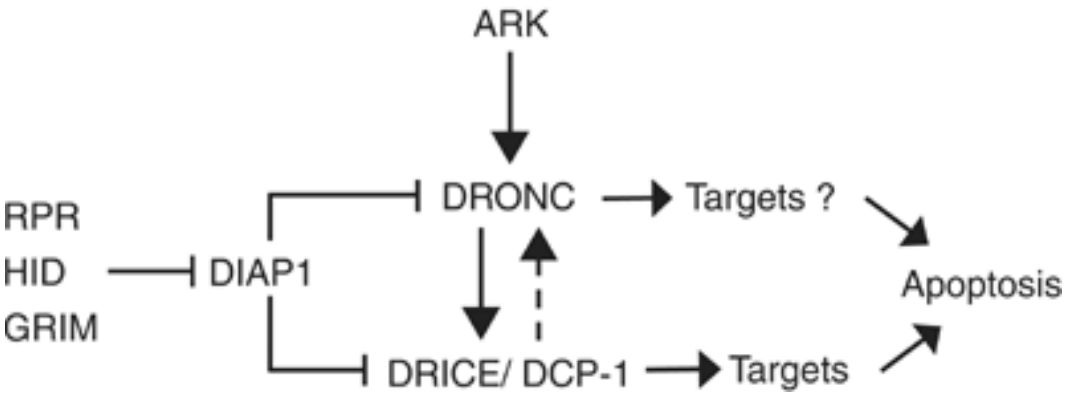

Figure 6. Apoptosis Pathway

DIAP1 regulates the activity of caspases DRONC and DRICE/DCP-1. The Apaf-1 domain ARK activates DRONC, which further activates downstream effector caspase DRICE/DCP-1 and triggers apoptosis. RPR, HID, AND GRIM are IAP antagonists that can inhibit the anti-apoptotic activity of DIAP1 due to their high affinity for its binding sites (Kumar, 2007).

PCD in Larval Salivary Glands

The larval salivary glands are located in the ventro-lateral section of the posterior head (Denny et al., 1997). Larval salivary glands display apoptosis markers such as DNA fragmentation prior to their destruction. However, the appearance of autophagic vacuoles containing mitochondria and the spherical shape of the cells indicate that larval salivary glands are destroyed by autophagy during the second pulse of ecdysone at around 12 hr APF (Baehrecke, 2003). The second pulse of ecdysone induces the

cell death genes *rpr* and *hid,* whose gene products bind to DIAP1 and mark the latter for degradation in the larval salivary glands (fig. **7**) (Cao et al., 2007). However, *rpr* and *hid* alone cannot promote the degradation of DIAP1 in the salivary due to the high level of expression of the protein in early developmental stages. Larval salivary glands destruction is first mediated by the expression of CREB binding protein (CBP), which decreases the level of DIAP1 in the salivary glands at the mid third instar. At low level of expression, DIAP1 is subject to degradation by RPR and HID at the second pulse of ecdysone in salivary glands (Yin et al., 2007). In the absence of *hid*, the larval salivary glands fail to undergo PCD; thus, both *rpr* and *hid* are required for larval salivary glands degradation (Cao et al., 2007). Broad Complex (*BR-C), E74A,* and *E75A* are re-induced by the second pulse of ecdysone along with *E93* (Bond et al., 2011). The re-induction of the early genes and the expression of *E93* trigger PCD in the salivary glands. *E93*, *rpr*, and *hid* together, seem to regulate cell death in the larval salivary glands (Lee et al., 2002; Broadus et al., 1999).

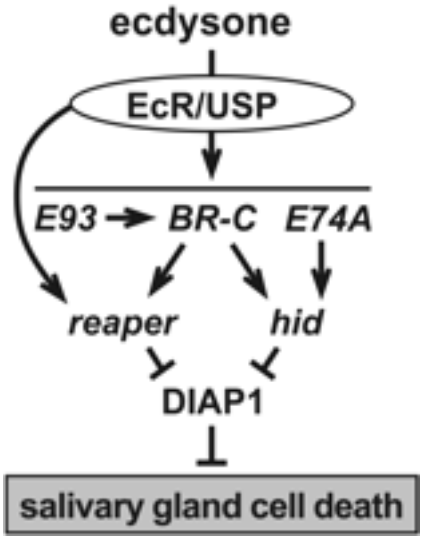

Figure 7. Regulation of the cell death genes in *Drosophila melanogaster* larval salivary glands by ecdysone. The second pulse of ecdysone induces both the early genes along with *E93* and the cell death genes *rpr* and *hid*, whose gene products inhibit DIAP1 in the larval salivary glands at around 12 hr APF. Hence, the salivary glands are destroyed (Cao et al., 2007; Bond et al., 2011).

Origin and Role of the *Drosophila* fat body

The *Drosophila* larval fat body arises from the inner ventral portion of the embryonic mesoderm and is developed in a longitudinal pattern with homologous segments next to each other. The location of tissues is controlled by homeotic genes, which determine the anterior-posterior and dorsal-ventral development of the mesoderm (Miller et al., 2002). Homeotic genes are expressed during the early stage of development and

code for specific spatial patterns in insects (Goodrich et al., 1997). The fat-body precursors are organized in a dorsal-ventral position and are composed of three distinct domains: lateral fat body, dorsal fat-cell projections, and ventral fat-cell commissure (Campos-Ortega and Hartenstein, 1997; Hoshizaki et al., 1994). The fat tissue completes its cellular division at the embryonic stage and the cells continue to grow throughout the larval period (Bate & Arias, 1993). The larval stage is a feeding period in which the larva grows rapidly and stores enough fat as energy supply for metamorphosis (Aguila et al., 2007).

Matrix Metalloproteinases (MMPs) and TIMPs

The Matrix Metalloproteinase (MMP) families of extracellular proteases are enzymes that cleave the extracellular matrix (ECM) of tissues during processes such as wound healing and tissue remodeling (Vu and Werb, 2000). The genome of *Drosophila* codes for two MMPs: MMP1 and MMP2. MMP1 is a secreted protease and MMP2 is a membrane-bound protease. MMP1 and MMP2 are both involved in tissue remodeling and PCD; nevertheless, they fulfill specific functions (Bond et al., 2011). MMP1 is required for the proper development of the trachea. MMP1 might also be involved in larval salivary glands cell death due to *mmp1* expression in this organ at the second pulse of ecdysone. MMP2, on the other hand, is involved in the histolysis and remodeling of larval

tissue such as the midgut and the fat body respectively (Bond et al., 2011; Page-McCaw, 2007).

The proenzyme form of MMPs is stabilized by the interaction of cysteine with calcium (Ca2+) and the zinc moiety of the enzyme active site. Upon cleavage of the N-terminus of the proenzyme, MMPs become reactive (Page-McCaw, 2007). The ECM of *Drosophila* is composed of type IV collagen, laminin, glutactin, and fibronectin. *Drosophila* type IV collagen corresponds to the type IV mammalian collagen (Fessler and Fessler, 1989). MMP1 can degrade the type IV collagen of mammalian and fibronectin while MMP2 degrades collagen, gelatin, and stromelysin (Llano et al., 2000). MMP2 differs from MMP1 by its rich C-terminus which contains an extension composed of acidic residues and a stretch of hydrophobic residues. In addition to the C-terminus modification, the specificity pocket of MMP2 allows binding of bulky proteins (Llano et al., 2002).

In addition to the MMPs, tissue inhibitors of metalloproteinases (TIMPs) are endogenous proteins that regulate MMPs at the inhibition or zymogen level in mammals and invertebrates. The N-terminal and C-terminal domains of mammalian TIMPs are stabilized by three disulfide bonds (Brew and Nagase, 2010). Humans possess four TIMPs which are: TIMP-1, TIMP-2, TIMP-3, and TIMP-4. However, *Drosophila melanogaster* genome codes for one TIMP, which lacks a disulfide bond (Cys^{13}-Cys^{124}) at

the N-terminal of the inhibitory domain compare to human TIMP-1 (Wei et al., 2003).

Drosophila **Fat Body Remodeling**

While the salivary glands of *Drosophila* undergo PCD during metamorphosis, the larval fat body is spared from PCD and is remodeled (Nelliot et al., 2006). The larval fat body is a sheet of connected polygonal cells that occupies most of the peripheral space between the body wall and the gut (fig. 8b). The matrix metalloproteinase enzyme (MMP2) cleaves the extra cellular matrix of the fat body, which is remodeled from anterior to posterior. MMP2 is expressed at around 10 hr APF in the fat body and triggers the catalytic cleavage of the extra cellular matrix (Nelliot et al., 2006). At around 6 hr APF, the fat cells from the anterior region begin to move closer to the abdominal region and become spherical (fig. 8a). At 12 hr APF, when head eversion occurs, the anterior fat cells are completely detached into single cells and are pumped to the head by muscular contractions. Around 14 hr APF, the fat cells are completely remodeled (Nelliot et al., 2006; Bond et al., 2011). The fat body is transformed into free floating, individual spherical single cells to provide nutrients for the *Drosophila* during metamorphosis (fig. 8a). The fat cells are later destroyed by PCD 2 to 4 days in the adult fly and are replaced by a new fat body,

which also emerges from the mesoderm layer (Aguila et al., 2007; Bate & Arias, 1993).

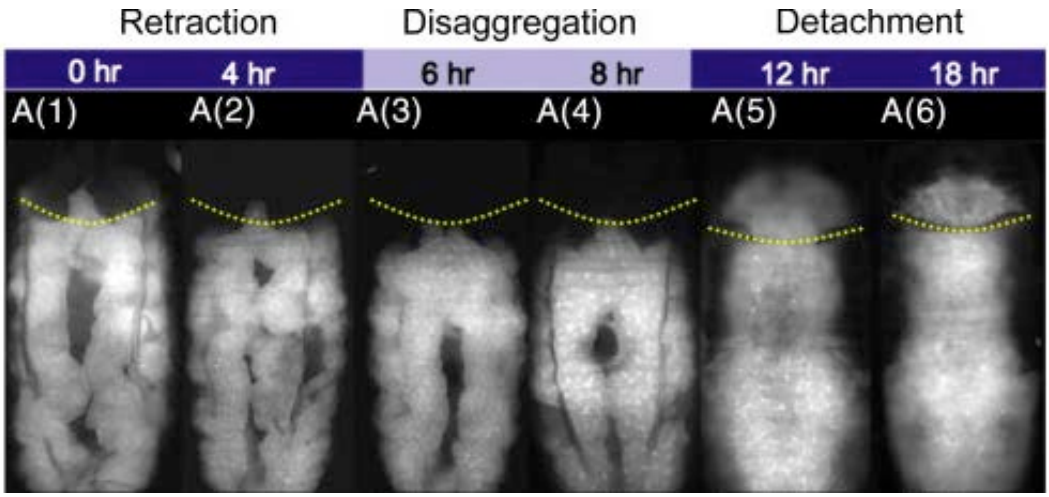

Figure 8a. Fat body remodeling in *Drosophila.* At around 0 hr APF, the fat body begins to retract in the abdominal cavity. All the fat body is packed in the abdominal cavity of the animal at around 6 hr APF and fat cells become spherical. At around 12 hr APF, the extra cellular matrix is cleaved and the single spherical cells are pumped to the head by muscular contractions (Bond et al., 2011; Nelliot et al., 2006)

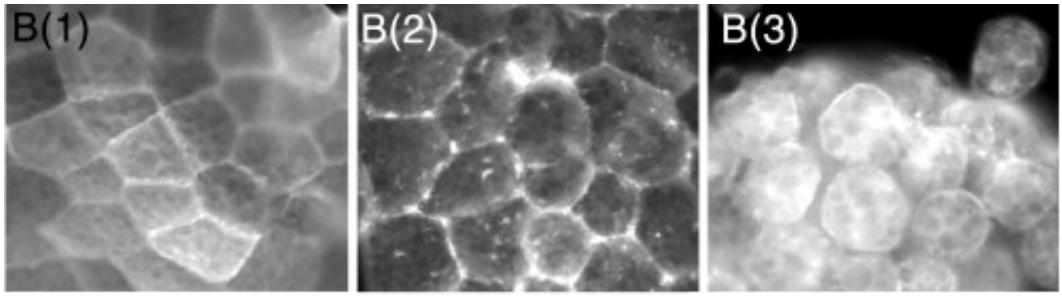

Figure 8b. Fat body remodeling during metamorphosis. The matrix metalloproteinase (MMP2) cleaves the extra cellular matrix of the fat body, which is a sheet of flat polygonal and connected cells. B(1) flat, polygonal, and connected cells of the fat body. B(2) The extra cellular matrix is cleaved by MMP2 and the fat cells gradually become spherical. B(3) Free single and spherical fat cells are visible (Bond et al., 2011)

Hypothesis

Several aspects of the genetic regulation of fat body remodeling in *Drosophila* are still not well understood. When the fat body undergoes remodeling at around 12 hr APF, some larval tissues such as the salivary glands undergo PCD through the down-regulation of *diap1* and the induction of the IAP antagonists: *rpr* and *hid*. *diap1* is an anti-apoptotic gene that down-regulates or delays the expression of pro-apoptotic genes (Jiang et al., 2000).

My research examines the expression of *diap1* in the fat body during metamorphosis. I hypothesize that *diap1* is expressed in the larval fat body throughout metamorphosis and this helps to inhibit PCD in this organ. To test this hypothesis, I examined *diap1* transcript levels in wild type *Drosophila* using quantitative Real Time PCR. In addition, I generated flies in which *diap1* expression is downregulated in the fat body by a *diap1 RNAi* construct. I used quantitative Real Time PCR to determine the expression of *diap1* of both control and *diap1 RNAi* animals at L3, 6 hr APF, 12 hr APF, and 14 hr APF. To examine the consequences of knockdown *diap1* expression on fat body development, I observed fat body in *diap1 RNAi* and control animals expressing green fluorescent protein (GFP) in the fat cells.

MATERIALS AND METHODS

Drosophila melanogaster stocks and crosses

For this project, flies with the genotypes w^{1118}, *LSP2-GAL4*, *LSP2::SYB*, and *UAS-diap1 RNAi* were maintained on a yeast medium supplemented with dry yeast at 25 °C. *UAS-diap1 RNAi* flies were obtained from the genetics department at Harvard Medical School. The *diap1 RNAi* construct was made by inserting a short hairpin that corresponds to the *thread* gene or *diap1* on the third chromosome of the fly (flyrnai, 2012). The top and bottom sequences of *diap1 RNAi* hairpin were as followed:

Top: ctagcagtCACCCAAGTCCTCAAATTCAAtagttatattcaagcataTTGA

ATTTGAGGACTTGGGTGgcg

Bottom: aattcgcCACCCAAGTCCTCAAATTCAAtatgcttgaatataactaTTG

AATTTGAGGACTTGGGTGactg

Plastic bottles containing *LSP2-GAL4, UAS-diap1 RNAi,* and *LSP2::SYB* larvae and pupa were cottoned and store at 25 °C or 18 °C. Virgins female and male *Drosophila* were collected separately at 8 hours or 18 hours after the fly became an adult and stored in plastic vials containing a yeast medium at 18 °C. Virgin females are not sexually active. Crosses were later made between male *LSP2-GAL4* and female *UAS-diap1 RNAi*; female *LSP2::SYB* and male *UAS-diap1 RNAi* collected virgins to

generate F1 progeny, in which *diap1* was down-regulated in the fat body. The reciprocal for each cross was also made.

GAL4 X UAS System

GAL4 is a useful system that enables the ectopic expression of a specific gene. In a GAL4 X UAS system, GAL4 is a driver expressed in the line of transgenic animals and UAS is a responder with a reporter gene expressed in another line of transgenic animals. GAL4 is a eukaryotic transcription factor derived from the yeast *Saccharomyces cerevisiae*. GAL4 activates the transcription of the genes *gal10* and *gal1* which are involved in galactose metabolism in yeast (Elliott and Brand, 2008). The GAL4 protein functions as a dimer with one domain that binds to a specific sequence on the DNA and another that activates RNA polymerase for the transcription of the reporter gene associated with GAL4 (Nelson and Cox, 2008). The GAL4 protein dimer binds to DNA through a Zn-Cys zinc finger at four specific sites composed of 17 base pairs. The four sites represent an upstream activation sequence (UAS) for the transcription of the reporter gene. The GAL4/UAS system is used for tissue-specific target gene expression in *Drosophila* and is highly conserved in eukaryotes (Elliott and Brand, 2008; Duffy, 2002)

In this project, the flies with the reporter gene were the *UAS-diap1 RNAi* and the flies with the driver were the *LSP2-GAL4* and *LSP2::SYB*

(fig. 9). The *LSP2::SYB* flies are the same as the *LSP2-GAL4* except that the gene coding for the green fluorescent protein (GFP) is bound to the driver. The progeny from the crosses of *LSP2-GAL4* and *UAS-diap1 RNAi* and *LSP2::SYB* and *UAS-diap1 RNAi* express the *diap1 RNAi* sequence, which is the reporter gene in the fat tissue.

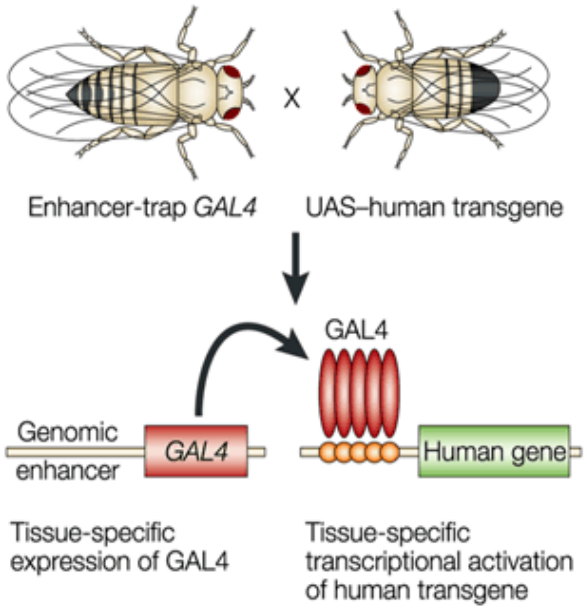

Figure 9. GAL4/UAS System in Drosophila. The enhancer-trap *GAL4* and the *UAS* -transgene are located on different chromosomes. In progenies from the enhancer-trap *GAL4* and the *UAS*-transgene crosses, the GAL4 protein binds to the *UAS* sequence and activates the transcription of the reporter human gene (Muqit and Feany, 2002; St Johnson, 2002).

RNA Interference Mechanism

RNA interference (RNAi) or post transcriptional gene silencing is a technique used to suppress gene expression in the study of gene functions. RNAi is accomplished by inserting a long or short double-stranded RNA (dsRNA) in cells or by overexpressing a hairpin dsRNAs in animals (Ling and Li, 2004; Kondo et al., 2009). The GAL4 system can be used to drive the transcription of the dsRNAs responder and knockdown gene expression in transgenic animals. When transcribed, the long dsRNA is cleaved into small interfering RNAs (siRNA) by a ribonuclease III enzyme or dicer and is converted into single stranded siRNAs or microRNA (miRNA) by RNA-induced silencing complex (RISC) (fig. 9). siRNA binds to a specific sequence of an endogenous mRNA that matches the sdRNA in cells and triggers the activation of RNases for the degradation of the target mRNA(Yu et al., 2002; Paroo et al., 2007; Tijsterman and Plasterk, 2004). Gene silencing events occur naturally in the cells of almost all eukaryotes such as flies, nematodes, insects, and human during development and involve miRNAs (Agrawal et al., 2003). The *Drosophila* genome codes for two dicers, Dcr-1 and Dcr-2. Dcr-1 triggers gene silencing through miRNA and Dcr-2 produces enzymes involved in this process (Tijsterman and Plasterk, 2004). In mammals, RNAi is evolutionary conserved and confers resistance against foreign pathogens and endogenous parasites (Ling and Li, 2004).

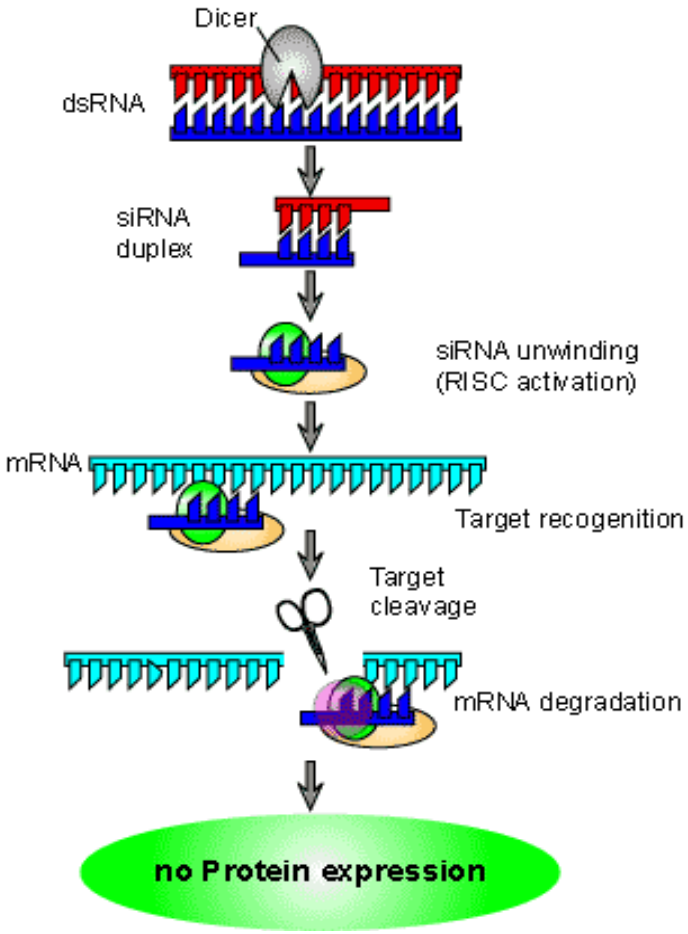

Figure10. RNA interference mechanism. The dsRNA is transcribed and is cleaved into siRNA by a dicer, which is a ribonuclease III enzyme. The single stranded siRNA binds to the target mRNA at a specific sequence and triggers the degradation of this mRNA (picture retrieved from vet.uga.edu; Paroo et al., 2007; Tijsterman and Plasterk, 2004).

RNA Isolation and DNase Treatment

Wild type *w^{1118} and diap1 RNAi* flies were aged to L3, 6 hr, 12 hr, and 14 hr APF at 25 °C and dissected under the dissecting microscope. Fat body was collected from 4 to 6 animals in 1.5 mL tubes containing 30 µL of 1X PBS buffer solution. 300 µL trizol was added to mixtures to lyse the fat cells. The tubes were stored at -80 °C for RNA isolation.

The trizol solutions containing RNA from the fat body were later transferred to a 2 mL phase lock gel-heavy tubes and 60 µL of chloroform was added to the mixtures. The phase lock gel-heavy tubes were centrifuged for 10 minutes at 12,000 rpm and the clear phase was collected in clean RNase free tubes and mixed with 160 µL of isopropanol. The samples were stored at -20 °C for overnight RNA precipitation. The next day, the samples were washed with 75% alcohol to collect the pellet. The pellets were redissolved in 11 µL of nuclease free water. 1 uL was taken from each sample for RNA quantification using the ThermoScientific Nanodrop 2000c spectrophotometer. A high quality RNA has a ratio of absorbance at 260nm to 280nm between 1.95 and 2.

A DNase treatment was performed to remove contaminating genomic DNA from the isolated RNA. 1 µL of 10X DNase buffer and 1 µL of r-DNase were added to each 10 µL of RNA followed by 25 to 30 minutes incubation at 37 °C. After incubation, 2 µL of pre-vortexed DNase Inactivation Reagent was added to each sample. The samples were

incubated at room temperature for 2 minutes and spun at 10,000 rpr for 90 seconds. The clear supernatant was then transferred to a new RNase-free tube. The DNase treatment was repeated with 1.5 µL of 10X DNase buffer instead of 1 µL and the measurements were the same for the rest of the protocol. After the DNase treatment, the concentration and ratio of absorbance of the samples were quantified. The concentrations ranged from 647 ng/µL to 148 ng/µL. The absorbance ratios at 260nm to 280nm were between 1.5 and 1.79.

Reverse Transcription

Reverse transcription is a molecular biology technique used to convert single stranded RNA into complementary DNA (cDNA) using the reverse transcriptase (RT) enzyme. Clean 1.5 mL RNA free tubes were labeled RT and no RT. A first master mix for n+1 samples (with n representing the number of samples) was prepared with the following reagents: oligo dT, 10 mM dNTPs, and DEPC treated water in a clean 1.5 mL RNA free tube. RNA was added last to each tube containing an equal amount of the master. The samples were incubated at 65 °C for 5 minutes. A table with the measurements is shown below.

Table1. Reverse Transcription Reaction mixture 1

Reagents	Volume (ul) / sample
10 mM dNTPs	1 µL
Oligo dT	1 µL
DEPC treated water	7 µL

A second master mix was prepared with 10X RT buffer, 25 mM $MgCl_2$, 0.1M DTT, and RNase Out in a clean 1.5 mL RNA free tube. 9 µl of the master mix was added to each sample. The reagents were added according to the table shown below. The samples were then incubated at 42 °C for 2 minutes.

Table2. Reverse Transcription Reaction mixture 2

Reagents	Amount per sample
10X RT buffer	2 µL
25 mM $MgCl_2$	4 µL
0.1 M DTT	2 µL
RNase Out	1 µL

After incubation, 1 µL of SuperScript II RT was added to each RT samples and 1 µL of DEPC treated water was added to the noRT samples. The samples were then incubated at 42 °C for 50 minutes followed by 70 °C for 15minutes. The samples were kept on ice for at least 1 minute and 1 µL of *E .coli* RNase H was added to each sample. A final incubation

at 37 °C for 20 minutes was performed before storing the samples at -20 °C for RT polymerase chain reaction (PCR).

Polymerase Chain Reaction

Polymerase Chain Reaction (PCR) was performed to amplify the synthesized cDNA. PCR amplifies a DNA sequence or template through a series of repeated thermal cycling. PCR involves three steps, denaturation, annealing, and extension, which last 30 seconds each. During the denaturation step, the double stranded cDNA template is heated to 94 °C and separates into two single strands (denaturation or melting). The forward and reverse primers each anneal to a segment of the single strand (annealing). The reaction is cooled to 72 °C and the heat resistant Taq DNA polymerase (enzyme) adds nucleotides to synthesize a new strand, which corresponds to the single cDNA template (extension). The newly synthesized copy and the template form a double stranded DNA (fig. 11). These three steps are repeated for 35 cycles or more and a final extension step, which last 5 minutes occurs at 72 °C.

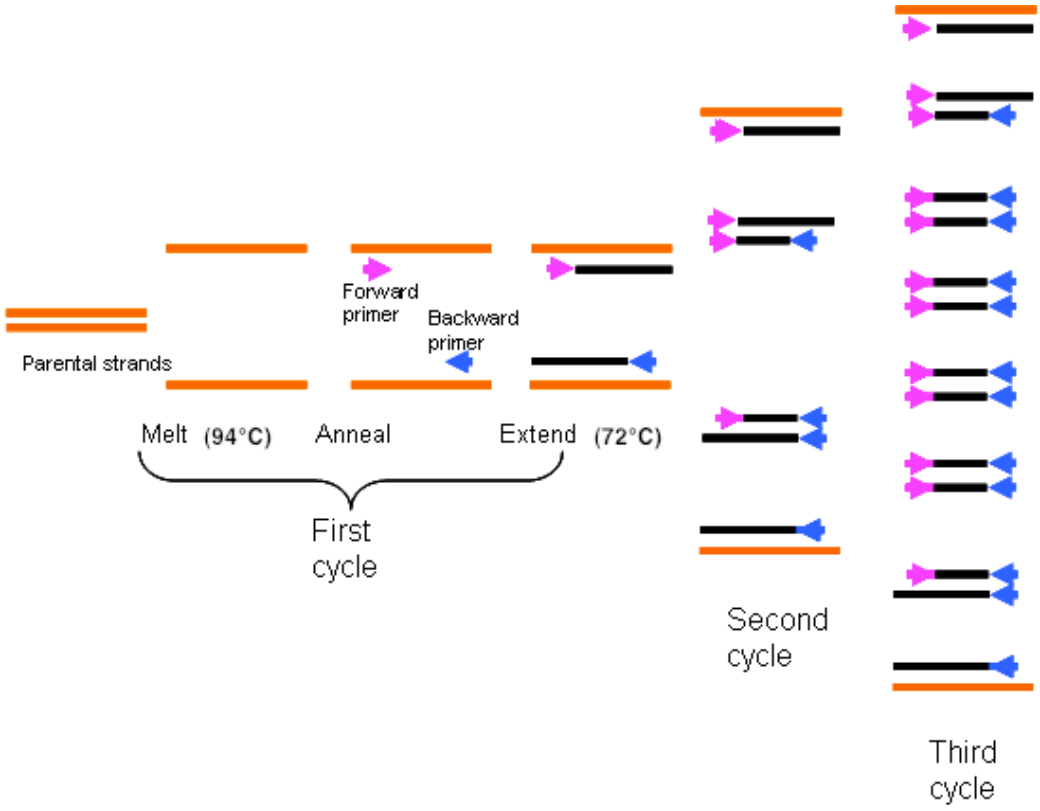

Figure 11. Polymerase Chain Reaction (PCR)
During the first cycle, the parental strands are denatured at 94 °C. The forward and backward primers anneal to the single strands at a specific temperature depending on the size of the primers. The reaction cools to 72 °C and nucleotides are added to generate two new strands of DNA. During the second cycle, the same process is repeated for the two double stranded DNA that are generated during the first cycle. At the end of the second cycle, four double stranded DNAs are generated. At the end of the third cycle, eight double stranded DNAs are generated. The amount of full length products increases exponentially at each cycle (picture retrieved from obgynacademy.com; Nelson and Cox, 2008).

Primer Design

Forward and reverse primers were designed for both *Actin 5C* and *diap1* using the gene sequences from FlyBase. *Actin 5C* is a housekeeping gene expressed in all cells of animals during development (Bond and Davidson, 1986). The *diap1* forward and reverse primers were design to correspond to a segment on the *diap1* mRNA sequence. The sequences of the forward and reverse primers for *diap1* were as followed:

Forward: 5′-TGG CCT GCG CCA AGT GCG C-3′

Reverse: 5′-AGC TGG CCG TTG CGA TCG CC-3′

The sequences for the forward and reverse primers for *Actin 5C* were:

Forward: 5′-TCT ACG AGG GTT ATG CCC TT-3′

Reverse: 5′-GCA CAG CTT CTC CTT GAT GT-3′

The expected size of the *diap1* band and the *Actin 5C* band were 217 base pairs and 158 base pairs respectively. The primers were diluted to 500 μM, then to 10 μM with nuclease free water for PCR.

Reverse Transcriptase Polymerase Chain Reaction (RT-PCR)

A master mix for n+ 1 sample was made with 10X RT PCR buffer, 25 mM $MgCl_2$, 10 mM dNTPs, 10 µM forward primer, 10 uM reverse primer, and nuclease-free water. Taq polymerase was added last to the master mix. Table 3 displays the reaction mixture and the order in which the reagents were added for the master mix. 2 µL of cDNA was later added to each sample separately. The annealing temperatures for *Actin 5C* and *diap1* were 60.2 °C and 65.9 °C respectively. Table 4 represents a thermocycler profile for *diap1* RT-PCR. An agarose gel electrophoresis was later run to detect the expression of *diap1* and *Actin 5C* in the PCR products.

Table 3. RT-PCR Reaction Mixture

Reagents	Amount per reaction
10X RT PCR buffer	5 µL
25 mM $MgCl_2$	6 µL
10 mM dNTPs	1 µL
10 µM forward primer	2 µL
10 µM reverse primer	2 µL
Nuclease-free water	31.6 µL
Taq polymerase	0.4 µL

Table 4. Thermocycler profile for *diap1* RT-PCR

Stage	Temperature	Time per cycle	Cycle count
Denaturation	94 °C	30 sec	35 cycles
Annealing	65.9 °C	30 sec	
Extension	72 °C	30 sec	
Final extension	72 °C	5 min	1 cycle
Final hold	4 °C	-	-

Agarose Gel Electrophoresis

A 1.6% agarose gel was prepared to visualize the PCR products. 2.4g of agarose was added to a beaker containing 150 mL of 1X TAE buffer. The mixture was heated in the microwave until all the agarose was dissolved and 5 µL of Ethidium bromide (EtBr) was added to it. EtBr can intercalate in between DNA base pairs and fluorescences under the UV light. 1 µL of gel loading buffer containing bromophenol blue was added to each sample as a standard tracking dye for the gel electrophoresis. 13 µL of 100 base pairs ladder and 20 µL of PCR product per sample were loaded on the gel. An additional 10 µl of EtBr was added to the reservoir filled with 1X TAE buffer. The gel was run 35 minutes at 116 Volts. The gel image was captured under the Fujifilm LAS-3000 Luminescence Image Analyser.

Qualitative Real Time PCR (qPCR)

Quantitative Real time PCR (qPCR) was performed to detect the level of expression of *diap1* in both wild type and transgenic animals. A basic PCR reaction can be divided into three phases:

Exponential: The products are doubled and accumulate at the end of each cycle.

Linear: The reaction slows down as the reaction components are depleted; products start to degrade.

Plateau: The reaction has reached the end point and no more products are generated.

Conventional PCR uses agarose gel to measure the amplification of the cDNA at the plateau. If left for a long time, some of the PCR products begin to degrade as the reaction reaches the plateau phase (Applied Biosystems, 2012). However, qPCR measures the amplification of the cDNA at the exponential level when the reaction components are abundant (Applied Biosystems, 2012). The amplification of the cDNA is monitored by fluorescent reporter molecules such as SYBR Green I, Molecular Beacon or TaqMan probes during the cycles (Bustin, 2005). As the amount of products accumulates after a couple of cycles, the fluorescent dye increases. When the level of fluorescence reaches a

measurable level and crosses the threshold line, it generates a cycle threshold (Ct). This Ct value is used to quantify the expression of the cDNA (Applied Biosystems, 2012).

qPCR can be used for relative or absolute quantifications. Relative quantification measures the expression of a target gene versus a reference gene. Absolute quantification generates internal or external calibration curves (Pfaffl, 2001). Relative quantification was used for this project because we were measuring the level of expression of *diap1* in both wild type and *diap1 RNAi* animals. The SYBR GREEN fluorescent I dye was provided by the 5 Prime Company.

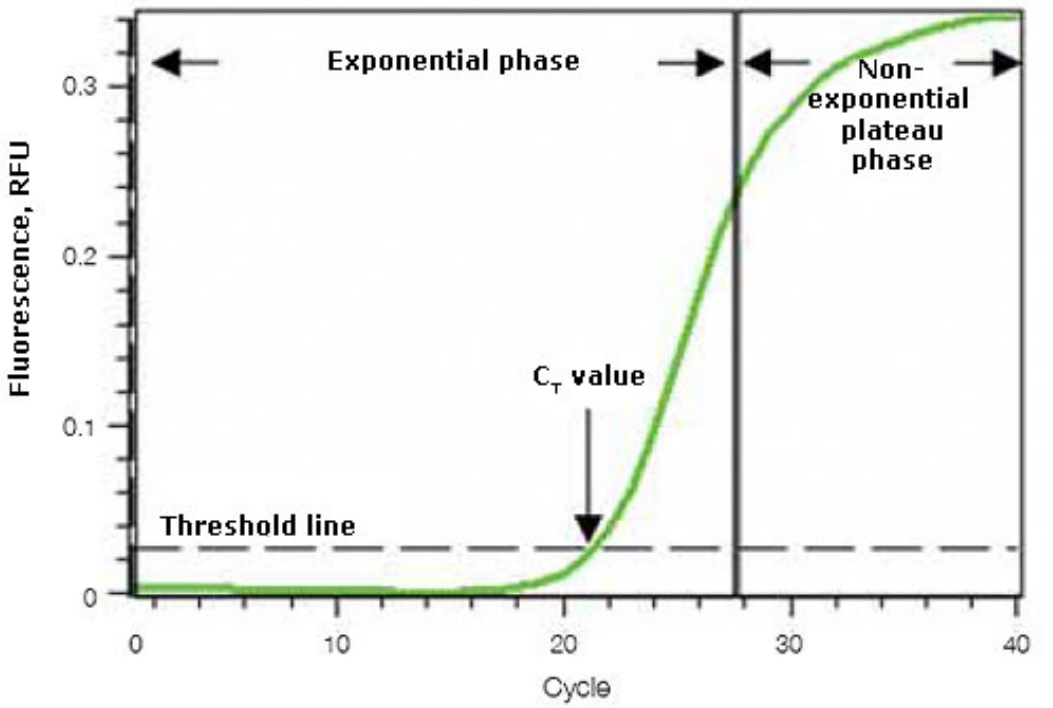

Figure 12. Qualitative Real time PCR
PCR includes three phases, exponential, linear, and plateau. qPCR uses fluorescent dyes such as SYBR green to detect the expression of a gene at the exponential phase. When enough products accumulate, the level of fluorescence increases and crosses the threshold line. As a result, a cycle threshold (Ct) value is recorded. The level of expression of a gene is calculated based on the Ct value. The lower the Ct value, the higher the concentration of the cDNA (retrieved from bio-rad.com; Bustin, 2005).

Primer Optimization and Standard Curves

A primer optimization assay was conducted for *diap1* using three different concentrations (300nM, 400nM, and 500nM) of both forward and reverse primers to determine the combination that generated the lowest Ct value. The cDNA used for the primer optimization assay was from RNA that was isolated from 5 whole animals that were aged for 12 hr APF. A

master mix was made for n+ 1 sample with 2.5 RealMaster mix Sybr Rox/ 20X Sybr solution, Nuclease Free water, and cDNA. The forward and reverse primers were added last according to their concentrations. A master mix for qPCR is represented in table 5.

Table 5. qPCR Reaction Mixture for primer optimization

Reagents	Amount per reaction
2.5 RealMaster mix Sybr Rox/ 20X Sybr solution	11.25 µL
Nuclease Free water	6.25 µL
cDNA	2.5 µL

Table 6. Thermocycler profile for *diap1* qPCR

Stage	Temperature	Time per cycle	Cycle count
Taq activation	95 °C	2 min	1
Denaturation	95 °C	15 sec	40
Annealing	60.2 °C	1 min	
Extension	72 °C	1 min	
Dissociation	95 °C →60 °C → 95 °C →60 °C	15 sec→1min→ 15 sec→15sec	1

Next, standard curves were generated to calculate the efficiency of the cDNA. A series of two fold dilutions of the cDNA (1, 1:1, 1:2, 1:3, 1:4) corresponded to 267 ng/µL, 133.5 ng/µL, 66.75 ng/µL, 33. 8 ng/µL, and

16.9 ng/µL. The log of the concentration of cDNA was plotted against the Ct values to generate a negative slope. The efficiency of the cDNA was then calculated using this equation Efficiency = $10^{-1/\text{slope}}$. A slope of -3.32 gives a perfect efficiency of 2 (Pfaffl, 2001).

Experimental qPCR

An experimental qPCR was performed for both wild type w^{1118} and *diap1 RNAi* animals to determine the relative expression of the target gene *diap1* in comparison to the reference gene *Actin 5C* in the fat body. The reactions were run in duplicate on 96-well plate for *Actin 5C* and *diap1* using RT, noRT samples from L3, 6 hr, 12 hr, and 14 hr APF, and no template control samples (NTC). New standard curves were generated for every experimental qPCR. Water was added to the NTC wells instead of cDNA. A master mix was made for n+ 1 sample with 2.5 RealMaster mix Sybr Rox/ 20X Sybr solution, Nuclease Free water, forward primer, and reverse primer. 2.5 µL of cDNA was added last to each well. The concentration of the cDNA from the fat tissue for w^{1118} and *diap1 RNAi were* 20 ($\pm$ 2) ng/µL.

Table 7. Experimental Qpcr Reaction Mixture

Reagents	**Volume per reaction**
2.5 RealMaster mix Sybr Rox/ 20X Sybr solution	11.25 µL
Nuclease Free water	6.25 µL
Forward Primer	2.5 µL
Reverse Primer	2.5 µL

The relative expression ratio of *diap1* to *Actin 5C* was calculated based on a new mathematical method, which uses only the efficiency of the target and reference genes and the ΔCt values (Pfaffl, 2001). The difference in the average Ct value for the target and reference genes was calculated using these equations:

ΔCt_{target} = control- transgenic

$\Delta Ct_{reference}$ = control –transgenic

The relative expression ratio *diap1* to *Actin 5C* at different developmental stages was calculated using this equation:

$$\text{Ratio} = \frac{(E_{target})^{\Delta Ct_{target}}}{(E_{reference})^{\Delta Ct_{reference}}}$$

In this equation, E is the efficiency calculated from the standard curves of the target gene and the reference gene.

Fluorescence Microscopy

Both control and *diap1 RNAi* animals expressing GFP were aged for 0 hr, 6 hr, 12 hr, and 24 hr APF and observed under the fluorescence microscope. Pictures of animals were taking under the UV light and they were pseudo-colored green.

RESULTS

Gel Electrophoresis

Gel electrophoresis was used to analyze the PCR products for the expression of *diap1* in the larval fat body at L3, 6 hr, 12 hr, and 14 hr APF. *diap1* was expressed in the larval fat body of both wild type and *diap1 RNAi* animals at all the developmental stages and amplicons of 217 base pairs were observed in the RT wells (fig. 13). A faint band could be observed in the RT well of L3 w^{1118}. No bands were observed in the noRT wells. Absence of bands in the noRT wells means that no genomic DNA was present in the noRT samples. The bands of primer dimers are remaining nucleic acids that didn't anneal during the conventional PCR reaction. However, no expression of *diap1* should be observed in the *diap1 RNAi* animals because the *diap1* construct was supposed to silence the transcription *diap1* in the fat body.

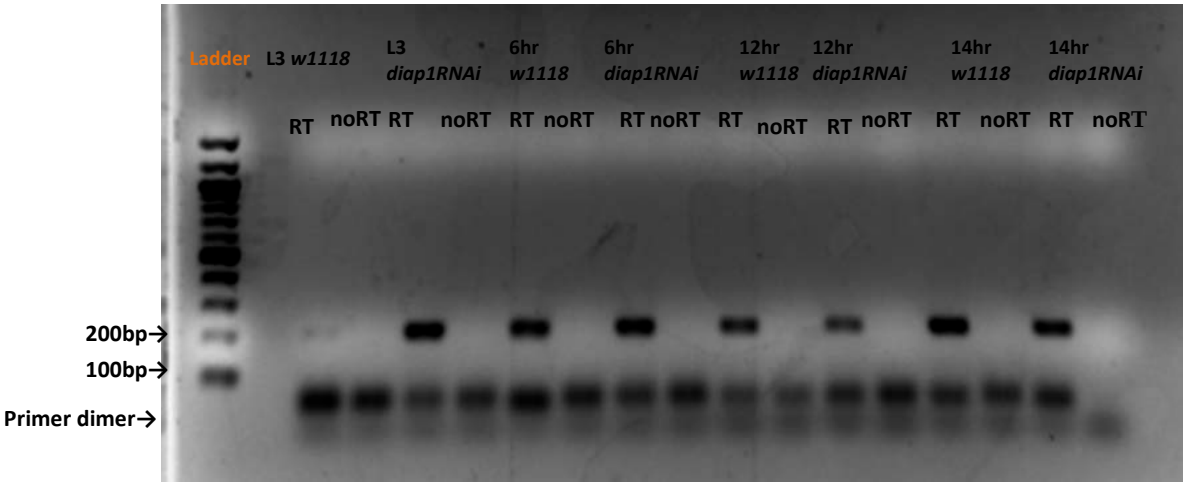

Figure 13. Expression of *diap1* in fat body of wild type w^{1118} and *Lsp2-gal4xUas-diap 1RNAi* animals at different developmental stages. *Diap1 RNAi* represents the *Lsp2-gal4xdiap1 RNAi* animals. w^{1118} was used as control. *diap1* was expressed in both wild type and *diap1 RNAi* animals. The RT wells means reverse transcriptase and the noRT means no reverse transcriptase. The primer dimers are remaining nucleic acids that didn't anneal during the PCR.

Standard Curves

The *diap1* primers were optimized with qPCR machine to determine the combination of forward and reverse primers concentration that would generate the lowest Ct value. From the combination of 9 reactions, the best ratio was 500nM forward and 500nM reverse with a Ct value of 17.06. Standard curves were then generated for *diap1* and *Actin 5C* to calculate the efficiency of the cDNA. The log of the concentration of the cDNA was plotted against the Ct values. *diap1* and *Actin 5C* generated negative slopes of -3.69 and -2.44 respectively. The efficiency of *diap1* was 1.87 and the efficiency of *Actin 5C* was 2.57. *diap1* effieciency was close to

the best efficiency value, which was 2. The efficiency of *Actin 5C* on the hand was higher.

a.

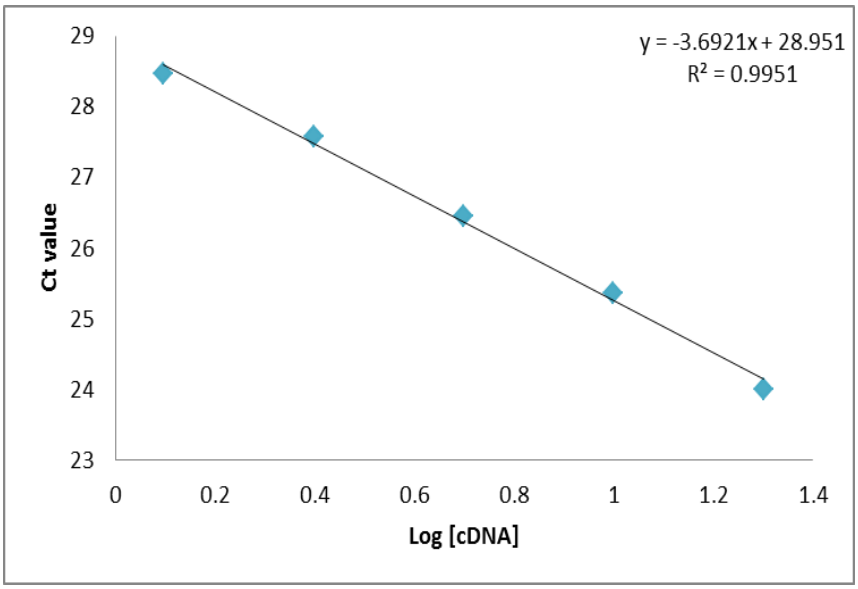

b.

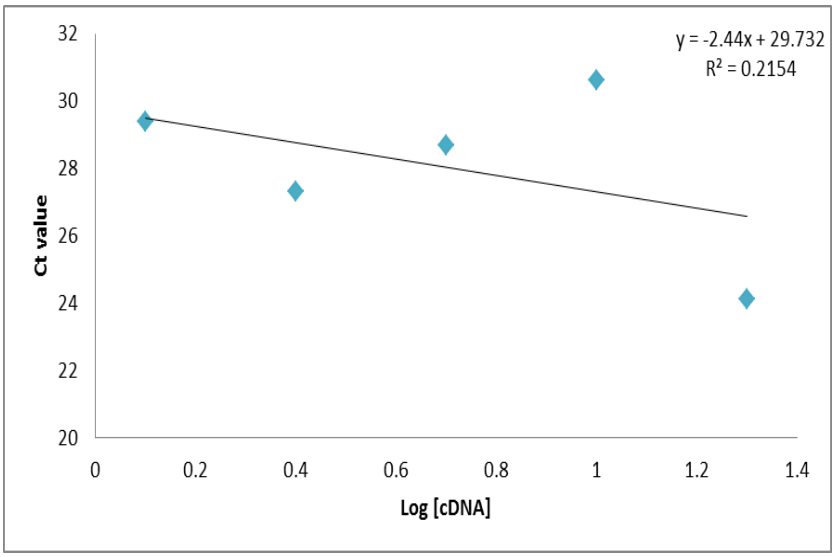

Figure14. Standard Curves of *diap1* and *Actin 5C*. The cDNA used for the standard curves was diluted through a series of two-fold dilutions. The standard curves were generated by plotting the log of the concentration of cDNA against the Ct values. The negative slope is used to calculate the efficiency of the primers. a and b represent the standard curve for *diap1* and *Actin 5C* respectively. Primers with an efficiency of 2 generate a slope of -3.32.

Experimental qPCR

The efficiency of *diap1* and *Actin 5C* primers were 1.87 and 2.57 respectively. Based on the Ct values for *w1118* and *diap1 RNAi* animals, relative expression of *diap1* in the *diap1 RNAi* compared to w^{1118} animals was determine at L3, 6 hr, 12 hr, and 14 hr APF. *diap1* decreased by 1.95 fold in L3, 0.66 fold at 6 hr APF, 1.7 fold at 12hr APF, and 1.85 fold at 14 hr APF. This decrease in the level of expression of *diap1* indicated that the *diap1* was down-regulated in fat body of the *diap1RNAi* animals.

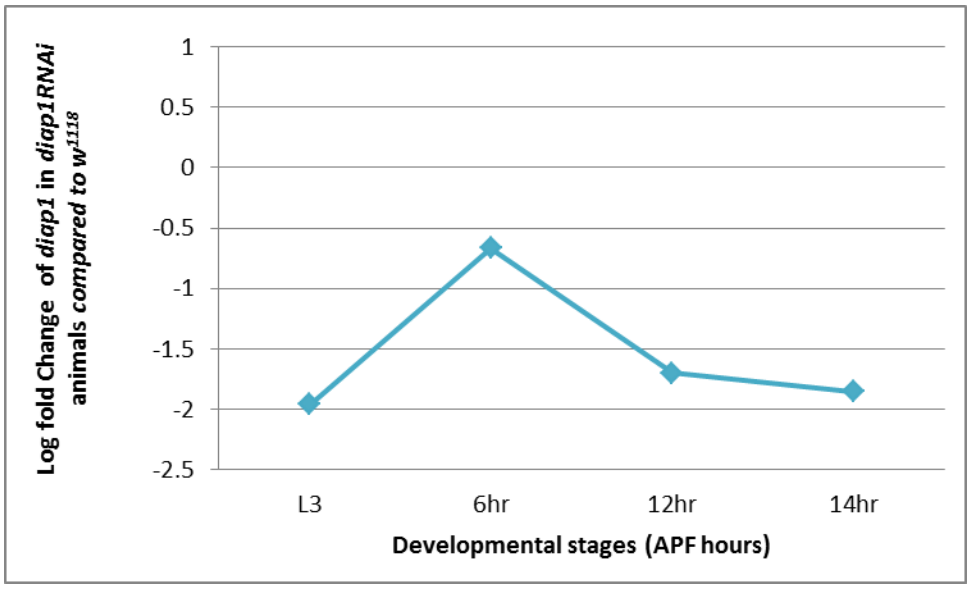

Figure 15. Relative Expression of *diap1 in diap1 RNAi* animals compared *to w1118* at different developmental stages. The ratio was calculated based on the new mathematical method that used only the efficiency of the primers. The developmental hours were plotted against the log of the ratio. The decrease in fold of *diap1* is less than 1 at all the developmental stages. A decrease in fold means that *diap1* was down-regulated in the larval fat body of the *diap1 RNAi* animals.

Fluorescence Microscopy

Fat body remodeling was observed in *Lsp2::syb x Uas-diap1RNAi* animals at 0 hr APF, 6 hr APF, 12 hr APF, and 14 hr APF. *Lsp2::syb* were used as control. At 0 hr APF, the fat body of both control and *diap1RNAi* animals was formed of connected cells, which already began to retract in the abdominal cavity (fig. 16). At 6 hr APF, the entire fat body was observed in the abdominal cavity of both control and *diap1RNAi* animals (fig. 17). However, at 12 hr APF, the fat cells were remodeled in the control and most of these individual fat cells were pumped to the head of the animal (fig. 18a). Even though individual fat cells were observed in the *diap1RNAi* animals, most of the fat tissue was still clustered in the abdominal cavity (fig. 18b). At 24 hr APF, fat body remodeling was complete in the control and fewer fat cells were observed (fig 19a). In the *diap1RNAi* animals, a cluster of fat tissue was still observed in the abdominal cavity (fig 19b). Pictures were taking for all the developmental stages with UV light. The pictures were pseudo-colored green because the fat body auto fluoresced when viewed under the GFP filter and less details could be noticed.

Figure 16. Fat body remodeling in *Lsp2::syb* and *Lsp2::syb x Uas-diap1 RNAi* animals at 0 hr APF. The red dotted lines depict the limit between the head and the abdomen of the animal. Sheets of fat tissue are observed laterally in the abdominal cavity of both *Lsp2::syb* (control) (16a) and *Lsp2::sybx Uas-diap1 RNAi* animals (16b). The fat tissue has also started retracting from to the abdomen. Scale bar = 98μm

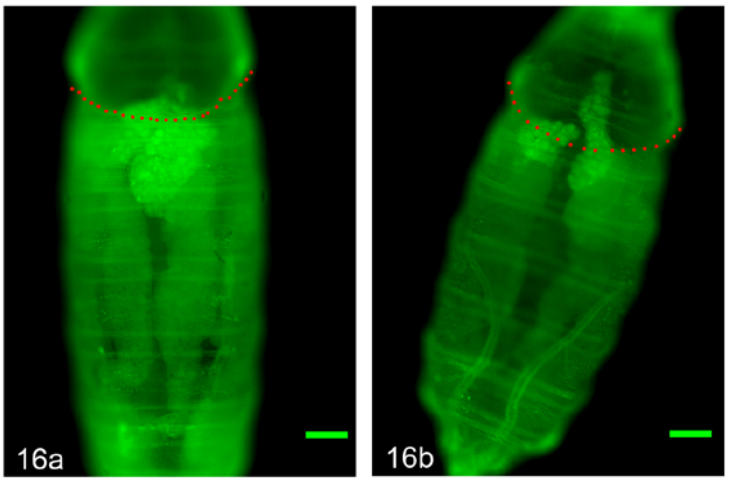
16a
16b

Figure 17. Fat body remodeling in *Lsp2::syb* and *Lsp2::syb x Uas-diap1 RNAi* animals at 6 hr APF. All the fat tissue was located in the abdominal cavity of both *Lsp2::syb* (17a) and *Lsp2::syb x Uas-diap1 RNAi* (17b). The fat cells in the anterior region of the abdomen are becoming spherical. Scale bar = 98μm

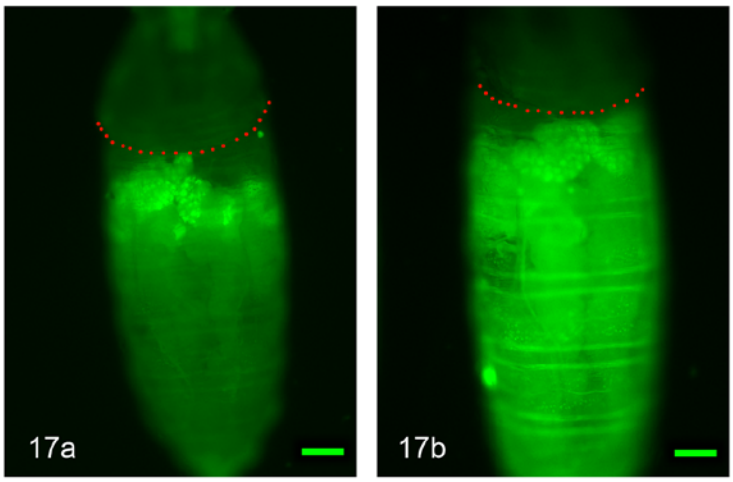
17a
17b

Figure 18. Fat body remodeling in *Lsp2::syb* and *Lsp2::syb x Uas-diap1 RNAi* animals at 12 hr APF. The fat body was remodeled in *Lsp2::syb* and most of the individual fat cells were in the head of the animal. In *Lsp2::syb x Uas-diap1 RNAi,* some of the fat tissue were remodeled. However, most of the fat body was clustered in the abdominal cavity of the animal. Scale bar = 98 μm.

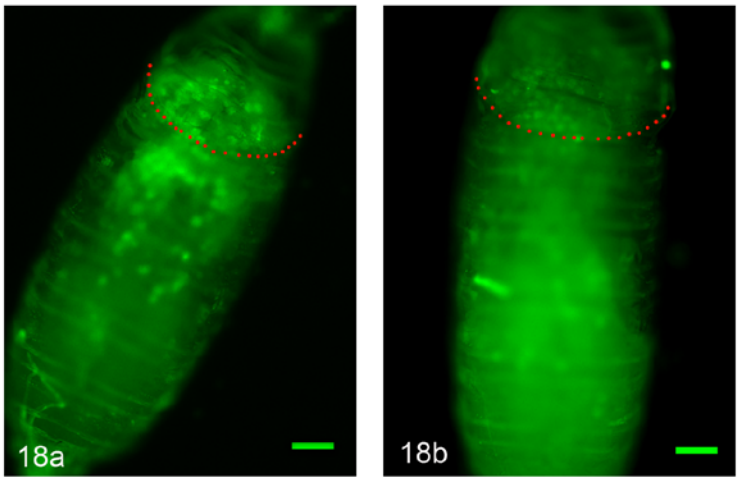
18a
18b

Figure 19. Fat body remodeling in *Lsp2::syb* and *Lsp2::syb x Uas-diap1 RNAi* animals at 24 hr APF. 19a. Complete fat body remodeling occurred in *Lsp2::syb*. Fewer fat cells are observed and they are concentrated in the head and anterior region of the abdomen of the animal. In 19b a cluster of fat cells are observed in the anterior portion of abdomen for the *Lsp2::syb x Uas-diap1 RNAi* animals. Clumps of fat are visible. Scale = 98μm.

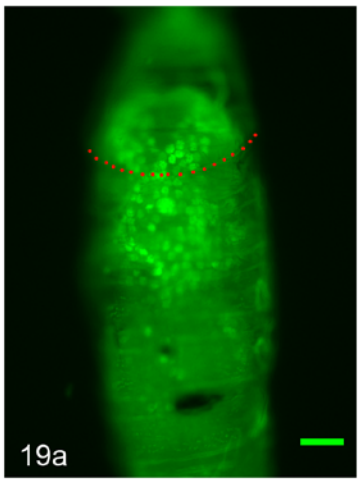
19a

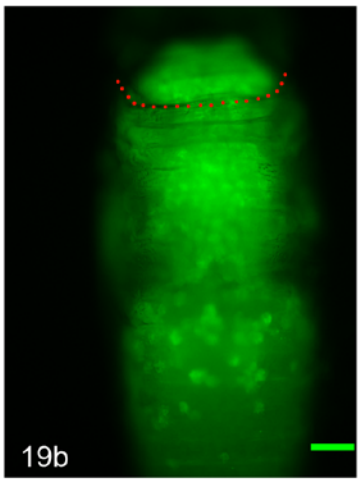
19b

DISCUSSION

In this project, I examined the role of *diap1* in fat body remodeling using real time PCR and fluorescence microscopy. Based on my results from my conventional PCR, *diap1* was expressed in the larval fat body of wild type and *diap1RNAi* animals at L3, 6 hr, 12 hr, and 14 hr APF. The evidence of *diap1* expressed in the larval fat body of my *diap1 RNAi* animals suggested that the construct might not be efficient at knocking down *diap1* in the fat tissue. Also, conventional PCR was only qualitative and not quantitative. If a small amount of *diap1* was present, PCR would still amplify the cDNA. Therefore I proceeded to qPCR to determine the relative expression of *diap1* in the fat tissue. I obtained an efficiency of 1.87 for *diap1* primer and an efficiency of 2.57 for *Actin 5C*. The efficiency of *diap1* was close to the perfect efficiency, which was 2. The efficiency of *Actin 5 C,* on the other hand excited the perfect value. Thus, *diap1* was more efficient at amplifying my cDNA than was *Actin 5C*.

My experimental qPCR generated higher Ct values for Actin 5C than diap1. The change in log fold of *diap1* in the *diap1 RNAi* animals compared to the wild type animals at the different developmental stages

were all below one. These negative values indicated that *diap1* was down-regulated in my *diap1 RNAi* animals.

In addition to my qPCR results, I made some interesting observations of my *Lsp2-gal4 x Uas-diap1 RNAi* animals while keeping the stock. After making crosses with male *Lsp2-gal4* and female *Uas-diap1RNAi*, I first noticed that they would take longer to lay eggs in comparison to the wild type and the *Lsp2::syb x Uas-diap1 RNAi*, second they would produce fewer progeny, and third, most of the F1 progeny would not survive metamorphosis. I further made the reciprocal and I observed the same pattern. The construct might not be knocking down *diap1* efficiently in the fat body yet, it was affecting the development of the fly.

My work with the fluorescence microscopy indicated that fat body remodeling was affected by the knockdown of *diap1* in the fat tissue. When I compared the control to the *Lsp2::syb x Uas-diap1 RNAi*, especially at 12 hr and 24 hr APF, fat body remodeling appeared different for each of them. Fat body remodeling is essential for the fly because energy and nutrients are released to support metamorphosis. If the fat tissue is not remodeled properly, metamorphosis can be delayed or arrested. In the

case of the *Lsp2::syb x Uas-diap1 RNAi*, fat body remodeling seemed to be delayed because this cross would generate more progeny, which survived metamorphosis.

My qPCR result supported my hypothesis. *diap1* was expressed in the larval fat body at L3, 6 hr, 12 hr, and 14 hr APF in the wild type and *diap1 RNAi* animals. However, there was a decrease in the level of expression of *diap1* in the transgenic flies compared to the wild type flies. The fact that most of the F1 progenies from *Lsp2-ga4x Uas-diap1 RNAi* animals died and that fat body remodeling didn't occur normally in the flies observed under the fluorescence microscope suggested that *diap1* is necessary for the normal timing of fat body remodeling and the successful development of *Drosophila*.

FUTURE DIRECTION

Additional work should be done about the role of *diap1* in fat body remodeling. Another student could work with some F2 progenies that survive in addition to the F1 progenies. One of my goals was to observe fat body remodeling in *Lsp2-gal x Uas-diap1 RNAi* in addition to my cross that expressed GFP. However, time didn't permit. Other students could observe fat body remodeling in *Lsp2-gal x Uas-diap1 RNAi* and monitor fat body remodeling by taking time lapse movies.

APPENDIX

Table 8. Experimental qPCR

Standard curves were constructed using 4 two fold dilutions of 12 hr APF whole animals (A and F). The expression of target (*diap1*) and reference (*actin 5C*) was measured using fat body cDNA samples from L3, 6 hr, 12 hr, and 14 hr APF. Cross represents the cDNA from *Lsp2-Gal4xUas-diap1 RNAi*. No template control (NTC) means that nuclease free water was added to those wells instead of cDNA.

	1	2	3	4	5	6	7	8	9	10	11	12
A	1 cDNA *Actin 5C*	1:1 cDNA *Actin 5C*	1:2 cDNA *Actin 5C*	1:3 cDNA *Actin 5C*	1:4 cDNA *Actin 5C*	NTC						
B	L3 *w1118* *Actin 5C*		6 hr *w1118* *Actin 5C*		L3 *w1118* *Actin 5C* noRT		6 hr *w1118* *Actin 5C* noRT					
C	12 hr *w1118* *Actin 5C*		14 hr *w1118* *Actin 5C*		12 hr *w1118* *Actin 5C* noRT		14 hr *w1118* *Actin 5C* noRT					
D	L3 Cross *Actin 5C*		6 hr *Cross* *Actin 5C*		L3 Cross *Actin 5C* noRT		6 hrCross *Actin 5C* noRT		L3 *w1118* *diap1* noRT		6 hr *w1118* *diap1* noRT	
E	12 hr *Cross* *Actin 5C*		14 hr *Cross* *Actin 5C*		12 hr Cross *Actin 5C* noRT		14 hr Cross *Actin 5C* noRT		12 hr *w1118* *diap1* noRT		14 hr *w1118* *diap1* noRT	
F	1 cDNA *diap1*	1:1 cDNA *diap1*	1:2 cDNA *diap1*	1:3 cDNA *diap1*	1:4 cDNA *diap1*	NTC						
G	L3 *w1118* *diap1*		6 hr *w1118* *diap1*		12 hr *w1118* *diap1*		14 hr *w1118* *diap1*		L3 Cross *diap1* noRT		6 hr Cross *diap1* noRT	
H	L3 *Cross* *diap1*		6 hr *Cross* *diap1*		12 hr *Cross* *diap1*		14 hr Cross diap1		12 hrCross *diap1* noRT		14 hr Cross *diap1* noRT	

Table 9. Primer optimization assay

Set up of the 96-well plate for *diap1* forward and reverse primers optimization assay. A combination of 9 reactions for the forward (300 nM, 400 nM, and 500 nM) and reverse primers (300 nM, 400 nM, and 500 nM) of diap1 were made to determine the best concentration ratio of primers that would generate the lowest Ct value.

	1	2	3	4	5	6	7	8	9	10	11	12
A	300: 300	300:400	300: 500	400: 300	400: 400	400: 500	500: 300	500: 400	500: 500			
B												
C												
D												
E												
F												
G												
H												

List of Abbreviations

APF = after puparium formation

BIR = Baculovirus IAP Repeat domain

bp = base pair

CARD = caspase recruitment domain

CBP = CREB binding protein

Ct= cycle threshold

dBRUCE= *Drosophila* BIR repeat containing ubiquitin-conjugating enzyme

DED= death effector domain

DIAP1= *Drosophila* inhibitor of apoptosis 1

dsRNA= double-stranded RNA

ECM= extracellular matrix

EcR = Ecdysone receptor

GFP= green fluorescent protein

JH= Juvenile hormone

L3 = third-instar larva

MMP= Matrix metalloproteinase

miRNA= microRNA

NBARC= nucleotide-binding adaptor shared by Apaf-1, certain R gene products, and CED-4

NTC = no template control

PCD = Programmed cell death

PCR = Polymerase Chain Reaction

PI3K = class I phosphoinositide 3-kinase

PTTH = Prothoracicotropic hormone

qPCR = Quantitative Real time PCR

RE = relative expression ratio

RGL = ring gland

RING = Really Interesting New Gene

RISC = RNA-induced silencing complex

RNAi = RNA interference

RT = reverse transcriptase

siRNA = small interfering RNA

TAE = tris-acetate EDTA

Taq = *thermus aquaticus*

TIMP = tissue inhibitor of metalloproteinase

TOR = Target of Rapamycin

Usp = Ultraspiracle

Literature Cited

Aguila JR, Suszko J, Gibbs AG, and Hoshizaki DK, 2007. The role of larval fat cells in adult *Drosophila melanogaster*. *J Exp Biol* 210:956-63.

Agrawal, N., Dasaradhi P. V. N., Mohmmed, A., Malhotra, P., Bhatnagar, R.K., and Mukherjee, S.K. 2003. RNA interference: biology, mechanism, and applications. *Microbiology and molecular biology reviews*. 6:.657–685.

Applied Biosystems. Real-time PCR vs. traditional PCR [online]. http:/www6.appliedbiosystems.com/support/tutorials/pdf/rtpcr_vs_tradpcr.pdf . Accessed on April 20, 2012.

Applied Biosystems. Real-time PCR: Understanding Ct. http://www3.appliedbiosystems.com/cms/groups/mcb_marketing/documents/generaldocuments/cms_053906.pdf . Accessed on April 22, 2012.

Baehrecke, E.H. 2003. Autophagic programmed cell death in *Drosophila. Cell Death and Differentiation.* 10: 940-945.

Baehrecke, E.H.(2005). Autophagy: dual roles in life and death? *Molecular Cell Biology*. 6: 505-510.

Bate, M., & Arias, A.M. 1993 The development of *Drosophila melanogaster* II. Cold Spring Harbor, New York.

Bio-rad gene expression. Real time PCR. http://www3. bio-rad.com/B2B/vanity/gexp/content.do?BV. Accessed April 22, 2012.

Bond, B. J. and Davidson, N. 1986. The *Drosophila melanogaster Actin 5C* gene uses two transcription initiation sites and three polyadenylation sites to express multiple mRNA species. *Molecular and Cellular Biology*. 6: 2080-2088.

Bond, N. D., Nelliot, A., Bernardo, M. K., Ayerh, M. A., Gorski, K. A., Hoshizaki, D. K., & Woodard, C. T. 2011. ßftz-f1 and matrix metalloproteinase 2 are required for fat-body remodeling in drosophila. *Devel. Biol*. 360 :286-296.

Brennan, C.A., Li, T., Bender, M., Hsiung, F., and Moses, K. 2001. *Broad Complex*, but not *Ecdysone receptor*, is required for progression of the morphology furrow in the *Drosophila* eye. *Development*. 128: 1-11.

Brew, K. and Nagase, H. 2010. The tissue inhibitors of metalloproteinases (TIMPs): An ancient family with structural and functional diversity. *Biochimica et Biophysica Acta.* 1803: 55-71.

Broadus, J., McCabe, J.R., Endrizzi, B., Thummel, C.S., and Woodard, C.T., 1999. The *Drosophila ßFTZ-F1* orphan nuclear receptor provides competence for stage-specific responses to the steroid hormone ecdysone. *Molecular Cell.* 3: 143-149.

Bustin, S. A. 2005. Real-Time PCR. *Encyclopedia of Diagnostic Genomics and Proteomics.* 1117- 1125.

Campos-Ortega, J. A. and Hartenstein, V. 1997. The embryonic development of *Drosophila melanogaster*. Springer-Verlag. New York.

Cao, C., Liu, Y., and Lehmann, M., 2007. Fork head controls the timing and tissue selectivity of steroid-induced developmental cell death. *The J. Cell Biol*. 176: 843-852.

Clarke, P. G. H.1990. Developmental cell death: morphological diversity and multiple mechanisms. *Anat. Embryol*. 181: 195-213.

Debnath, J., Baehrecke E.H., & Kroemer, G. 2005. Does autophagy contribute to cell death? *Landes Bioscience* 1: 66-74.

Demerec, M. (1950) Biology of *Drosophila*. Cold Spring Harbor, New York.

Denny, P.C., Ball, W.D., & Redman R.S. 1997. Salivary glands: a paradigm for diversity of glands development. *Critical Reviews in Oral Biology & Medicine.* 8: 51-75.

Diap1RNAi construct. http://www.flyrnai.org/TRiP-TTR-OVR.html. Accessed on March 28, 2012.

Duffy, J. B. 2002. Gal4 system in *Drosophila*: a fly geneticist's swiss army knife. *Genesis*. 34: 1-15.

Elliott, D.A. and Brand, A.H. 2008 The gal4 system: a versatile system for the expression of genes. *Methods Mol. Bio.* 420: 79-95.

Flymove. *Drosophila* life cycle. http://flymove.uni-muenster.de/accessed April 10, 2012.

Fessler J.H. and Fessler L.I., 1989. Drosophila Extracellular Matrix. *Ann Re Cell Biol* 5: 309-339.

Gavrieli, Y., Sherman, Y., & Ben-Sasson, S.A. 1992 Identification of programmed cell death in situ via specific labeling of nuclear DNA fragmentation. *The J. Cell Biol*. 119: 493-501.

Goodrich, J., Puangsomiee, P., Martin, M., Long, D., Meyerowitz, E. M., & Coupland, G. 1997. A Polycomb-group gene regulates homeotic gene expression in *Arabidopsis*. *Nature*. 386: 44-51.

Greenwood, D. R. and Rees, H.H. 1984. Ecdysone 20-mono-oxygenase in the desert locust, *Schistocerca gregaria. Biochemistry Journal*. 223: 837-847.

Hartenstein, V. 1993. Atlas of *Drosophila* development. Cold Spring Harbor.

Hoshizaki, D.K., Blackburn, T., Price, P., Ghosh, M., Miles, K., Ragucci, M., Sweis, R. 1994. Embryonic fat-cell lineage in *Drosophila melanogaster*. *Development*. 120: 2489-2499.

Jacobson, M. D., Weil, M., & Raff, M. C. 1997. Programmed cell death in animal development. *Cell*. 88: 347-354.

Jiang, C., Lamblin, A.F. J., Steller, H., & Thummel C.S 2000. A Steroid-Triggered Transcriptional Hierarchy Controls Salivary Gland Cell Death during *Drosophila* Metamorphosis. *Molecular Cell*. 5: 445–455.

Kanuka, H., Sawamoto, K., Inohara, N., Matsuno, K., Okano, H., and Miura, M., 1999. Control of the Cell Death Pathway by Dapaf-1, a *Drosophila* Apaf-1/ CED-4Related Capase Activator. *Molecular Cell*. 4: 757-769.

Kondo, S., Booker, M., and Perrimon, N. 2009.Cross-Species RNAi Rescue Platform in *Drosophila melanogaster*. *Genetics.* 183: 1165-1173.

Kumar, S. and Doumanis, J. 2000. The fly caspases. *Cell Death and Differentiation*. 7: 1039-1044.

Kumar, S. 2007. Caspase function in programmed cell death. *Cell Death and Differentiation*. 14: 32-43.

Lee, C.-Y., Wendel, D. P., Reid, P., Lam, G., Thummel, C. S. and E. H. Baehrecke. 2000. *E93* directs steroid-triggered programmed cell death in *Drosophila. Mol. Cell* 6: 433-443.

Lee, C. and Baehrecke, E.H. 2001. Steroid regulation of autophagic programmed cell death during development. *Development*. 128: 1443-1455.

Lee, C. Y., Simon, C. R., Woodard, C. T., & Baehrecke, E. H. 2002. Genetic mechanism for the stage- and tissue- specific regulation of steroid triggered programmed cell death in drosophila. *Developmental Biology*. 252:138-148.

Li, X., Wang, J., and Shi, Y. 2011. Structural mechanism of DIAP1 auto-inhibition and DIAP1 mediated inhibition of drICE. *Nature Communications*. 2: 408.

Ling, X. and Li, F. 2004. Silencing antiapoptotic survivin gene by multiple approaches of RNA interference technology. *BioTechniques*. 36: 450-460.

Llano E, Pendás AM, Aza-Blanc P, Kornberg TB, and López-Otín C, 2000. Dm1-MMP, a matrix metalloproteinase from Drosophila with a potential role in extracellular matrix remodeling during neural development. *J. Biol. Chem.* 275: 35978-85.

Llano E, Adam G, Pendás AM, Quesada V, Sánchez LM, Santamariá I, Noselli S, and López-Otín C, 2002. Structural and enzymatic characterization of Drosophila Dm2- MMP, a membrane-bound matrix metalloproteinase with tissue-specific expression. *J. Biol. Chem.* 277: 23321-9.

Maki, A., Sawatsubashi, S., Ito, S., Shirode, Y., Suzuki, E., Zhao Y., Yamagata, K., Kouzmenko, A., Takeyama, & K., Kato, S. 2004. Juvenile hormones antagonize ecdysone actions through co-repressor recruitment to EcR/USP heterodimers. *Biochemical and Biophysical Research Communications.* 320: 262-267.

Marino G. and Lopez-Otin, C. 2004. Autophagy: molecular mechanisms physiological functions and relevance in human pathology. *Cell. Mol. Life. Sci*. 61: 1439-1454.

McBrayer, Z., Ono, H., Shimell, M.J., Parvy, J. Beckstead, R.B., Warren J.T., Thummel, C.S., Dauphin-Villemant, C., Gilbert, L.I., & O'Connor, M.B. 2007. Prothoracicotropic hormone regulates developmental timing and body size in *Drosophila*. *Developmental Cell*. 13: 857-871.

Miller, J.M., Oligino T., Pazdera M., Lopez, A.J., and Hoshizaki D.K. 2002. Identification of fat-cell enhancer regions in *Drosophila melanogaster. Insect Molecular Biology*. 11: 67-77

Muqit, M.M.K. and Feany, B. 2002. Modeling neurodegenerative diseases in *Drosophila*: a fruitful approach? *Nature Reviews Neuroscience*. 3: 237-243.

Nelliot, A., Bond, N. and D.K. Hoshizaki. 2006. Fat-body remodeling in *Drosophila melanogaster*. *Genesis* 44: 396-400.

Nelson, D. L. and Cox, M. M. 2008. Lehninger principles of biochemistry. W. H. Freeman and Company. New York.

Obgyn Academy. PCR. http://www.obgynacademy.com/basicsciences/fetology/genetics/. Accessed April 22, 2012.

Orme, M. and Meier, P. 2009 Inhibitor of apoptosis proteins in *Drosophila*: gatekeepers of death. *Apoptosis*. 14: 950-960.

Page-McCaw, A. 2007. Remodeling the model organism: Matrix metalloproteinase functions in invertebrates. *Cell and Developmental Biology*. 19: 14-23.

Paroo, Z., Liu, Q., and Wang, X. 2007. Biochemical mechanism of the RNA-induced silencing complex. *Cell Research*. 17: 187-194.

Pfaffl, M.W. 2001. A new mathematical model for relative quantificationin Real time RT-PCR. *Nucleic Acids Research*. 29.

Riddiford, L. M. 1993. The Development of *Drosophila melanogaster,* Cold Spring Harbor Laboratory Press.

Riddiford, L.M., Hiruma, K., Zhou, X., & Nelson, C.A. 2003 Insight into the molecular basis of the hormonal control of molting and metamorphosis from *Manduca sexta* and *Drosophila melanogaster*. *Insect Biochemistry and Molecular Biology*. 33: 1327-1338.

Riddigord, L. (2008) Juvenile hormone action: A 2007 perspective. *J. Insec. Physiol.* 54: 895-901.

Schubiger, M., Wade, A.A., Carney G.E., Truman, J. W., & Bender, M. 1998. *Drosophila* EcR-B ecdysone receptor isoforms are required for larval molting and for neuron remodeling during metamorphosis. *Development*. 125: 2053-2062.

Scott.R.C., Schuldiner, O., and T. P. Neufeld. 2004. Role and regulation of starvation induced autophagy in Drosophila fat body. *Devel. Cell* 7:167-176.

St Johnson, D. 2002. The gal4-uas system for directed gene expression. *Nat. Rev. Gen*. 3: 176-188.

Tijsterman M., and Plasterk, R.H.A. 2004. Dicer at RISC: the mechanism of RNAi. *Cell*. 117: 1-4.

Thummel, C.S. 2007. To die or not to die−a role for Fork head. *J. Cell Biol* 17: 6737-739.

Vu, T. H., & Werb, Z. 2000. Matrix metalloproteinases: effectors of development and normal physiology. *Genes and Devel.* 14: 2123-2133.

Wei, S., Xie, Z., Filenova, E., and Brew, K. 2003. *Drosophila* TIMP Is a Potent Inhibitor of MMPs and TACE: Similarities in Structure and Function to TIMP-3. *Biochemistry*. 42: 12200-12207.

Woodard, C.T., Baehrecke, E.H., & Thummel, C.S. 1994. A molecular mechanism for the stage specificity of the drodophila prepupal genetic response to ecdysone. *Cell*, 79.

Yin, V. P. and Thummel, C.S. 2004. A balance between the diap1 death inhibitor and reaper and hid death inducers controls steroids-triggeres cell death in Drosophila. *Proc. Nat. Acad. Sci.* 101: 8022-8027.

Yin, V.P., Thummel, C.S., and Bashirullah, A. 2007. Down-regulation of inhibitor of apoptosis level provides competence for steroid-triggered cell death. *J.Cell. Biol.* 178: 85-92.

Yu, J-Y., DeRuiter, S. L., Turner, D.L. 2002. RNA interference by expression of short-interfering RNAs and hairpin RNAs in mammalian cells. *Proc. Nat. Acad. Sci.* 99: 6047-6052.